LBL-28045
Preprint

Lawrence Berkeley Laboratory
UNIVERSITY OF CALIFORNIA

Materials & Chemical
Sciences Division

Submitted to Journal of the Electrochemical Society

Current Distributions on Recessed Electrodes

A.C. West and J. Newman

November 1989

Prepared for the U.S. Department of Energy under Contract Number DE-AC03-76SF00098.

DISCLAIMER

LBL-28045

Current Distributions on Recessed Electrodes

Alan C. West and John Newman

Department of Chemical Engineering
University of California

and

Materials and Chemical Sciences Division
Lawrence Berkeley Laboratory
1 Cyclotron Road
Berkeley, CA 94720

LBL-28045

Current Distributions on Recessed Electrodes

Alan C. West[†] and John Newman

Materials and Chemical Sciences Division, Lawrence Berkeley Laboratory, and Department of Chemical Engineering, University of California, Berkeley, California 94720

November 14, 1989

Abstract

The primary current distributions on disk electrodes and two-dimensional electrodes that are recessed in insulating planes are given. The ohmic resistances are also given and are compared to previous estimates that were given in references [2] through [5]. A singular-perturbation analysis, valid for small aspect ratios, shows general behavior to be expected for all cells containing an electrode that is recessed slightly from the insulating plane.

Introduction

The primary current distributions and ohmic resistances of recessed, disk and planar electrodes are given. Recessed planar electrodes may be important, for example, for electroplating processes in the electronics industry. Recessed disk electrodes (see figure 1) may be designed to attain a fairly uniform current distribution on the disk [1]. They are also undoubtedly used because of an inability to construct disks that are perfectly coplanar with the insulating plane.

[†]Present Address: Département des matériaux, Laboratoire de métallurgie chimique, Ecole Polytechnique Fédérale de Lausanne, 34 chemin de Bellerive, 1007 Lausanne, Switzerland

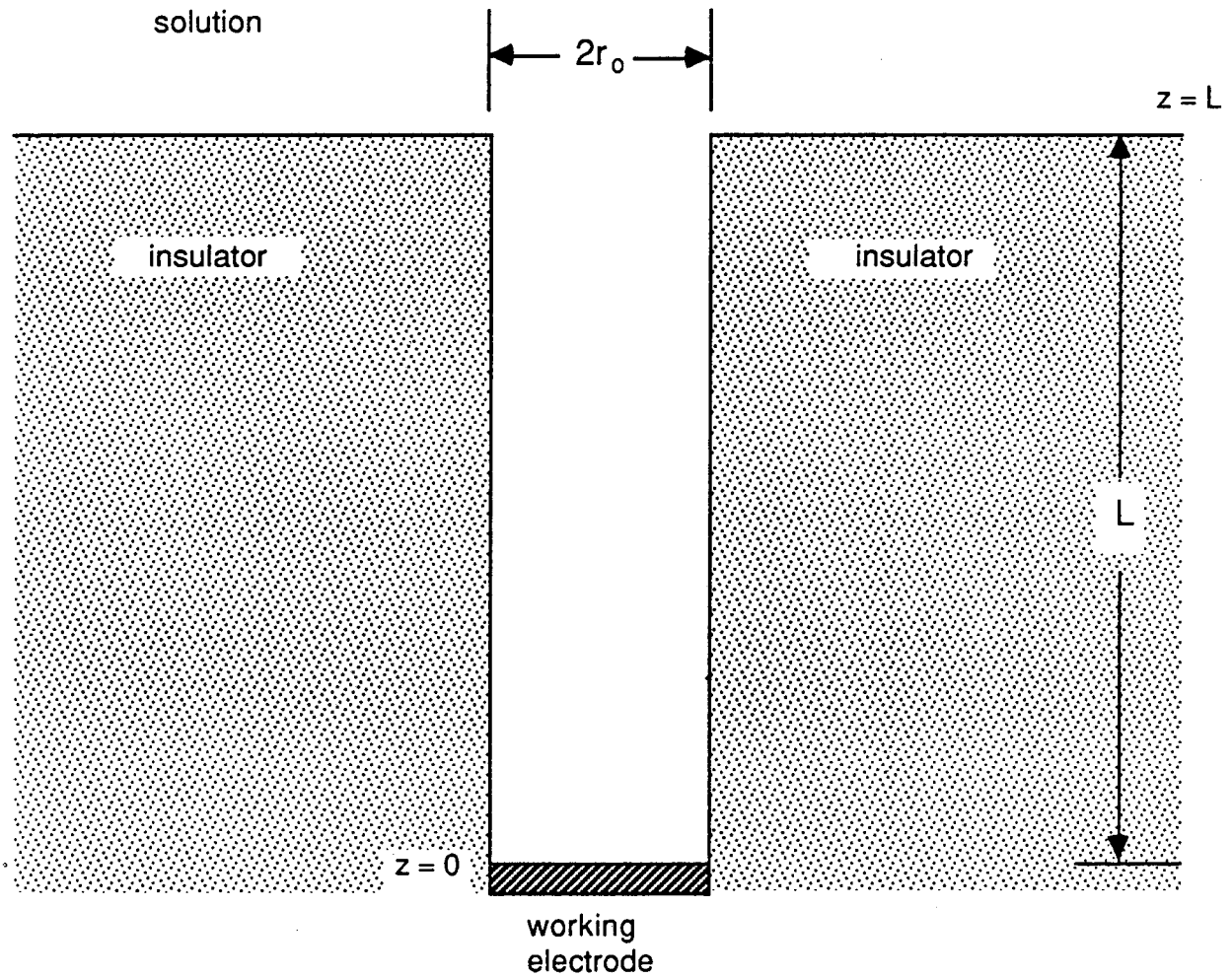

Figure 1. Schematic diagram of a recessed disk electrode.

The primary current distribution is valid when concentration variations are negligible and when the resistance of the interfacial reaction is zero. For these conditions, the distribution of current density and potential is given by Laplace's equation. The boundary conditions for the disk geometry are

$$\Phi = 0 \quad \text{as} \quad z^2 + r^2 \longrightarrow \infty, \tag{1}$$

$$\Phi = V \quad \text{at} \quad z = 0 \text{ and } r < r_o, \tag{2}$$

$$\frac{\partial \Phi}{\partial z} = 0 \quad \text{at} \quad z = L \text{ and } r > r_o, \tag{3}$$

and

$$\frac{\partial \Phi}{\partial r} = 0 \quad \text{at} \quad r = r_o \text{ and } 0 < z < L. \tag{4}$$

The outer radius of the insulating plane (at $z = L$) is assumed to be much larger than r_o.

Previous Work

As early as 1904, Maxwell [2] gave an approximate analysis that determined the ohmic resistance of a recessed disk electrode. He was unconcerned with the current distribution. Rayleigh [3] gave an approximate analysis, which resulted in an estimate of the mathematical equivalent to the ohmic resistance. In 1963, Kelman [4,5] investigated a steady-state diffusion problem that is the mathematical equivalent to the ohmic resistance.

The ohmic resistance R for current flow from the recessed disk to a counterelectrode at infinity can be given by

$$R\kappa r_o = \frac{1}{4} + \frac{L}{\pi r_o} + h_a(L/r_o). \tag{5}$$

The first two terms are the resistance of an isolated disk and the resistance of a circular cylinder. $h_a(L/r_o)$ is the explicit correction to the estimate of the resistance given by the other two terms. Maxwell [2] estimated an upper bound for $h_a(L/r_o)$ to be 0.02019, and Rayleigh [3] gave a refined estimate of the upper bound of 0.01235.

Kelman [4,5] gave a formal solution that utilizes Bessel functions for $z < L$ and Legendre polynomials for $z > L$. The coefficients of the two series were determined by matching at $z = L$ and $r < r_o$ the potential and the z derivative of the potential. He did not present the infinite series solution in a graphical form, so it is difficult to judge whether his solution converges in a finite number of terms.

Near $z = L$, $r = r_o$ (see figure 1), Laplace's equation can be solved to show that

$$\Phi(\rho,\theta) \propto \rho^{2/3}\cos(2\theta/3), \tag{6}$$

where ρ is the radial distance from the singular point and θ is the angular coordinate with $\theta = 0$ corresponding to $z = L$, $r > r_o$ and $\theta = \frac{3\pi}{2}$ corresponding to $r = r_o$, $z < L$. This implies that along the mouth of the pore,

$$\lim_{r \to r_o} \frac{\partial \Phi}{\partial z} \propto \rho^{-1/3}, \tag{7}$$

which is singular at $r = r_o$. A corresponding behavior for the radial derivative of potential prevails on the insulating plane near the opening.

We can ask whether Kelman's two series can give this behavior. Inside the pore, his expression for the current density at $z = L$ can be written as

$$\frac{\partial \Phi}{\partial z} = A_o + \sum_{n=1}^{\infty} A_n J_o(\alpha_n r/r_o). \tag{8}$$

Since the Bessel functions $J_o(x)$ are well-behaved, it is difficult for this series to converge for all $r \neq r_o$ and still to give the correct asymptotic behavior near $r = r_o$.

In the outer region, his expression for the current density can be written as

$$\frac{\partial \Phi}{\partial z} = \frac{1}{\eta} \sum_{n=0}^{\infty} B_n P_{2n}(\eta), \tag{9}$$

where $\eta = (1 - r^2/r_o^2)^{1/2}$. Since the $P_{2n}(\eta)$ are well-behaved, equation (9) is also unlikely to converge for all $r \neq r_o$ and to give the correct asymptotic behavior near $r = r_o$. Note that, when $L/r_o = 0$, the nature of the singularity changes, and the solution is valid because the term multiplying the summation goes to infinity in the correct manner as $r \longrightarrow r_o$.

The above discussion indicates that Kelman's solution should be viewed with caution because it does not deal with the singular behavior in a natural way. This does not imply that his results should be completely disregarded because numerical solutions that are clearly in error near a singular point have been observed to be approximately correct over the remainder of the domain.

Kelman [4,5] gave three asymptotic formulae, valid for different ranges of L/r_o, that can be used to estimate the cell resistance. These

formulae, when expanded, predict that $h_a(L/r_o) \rightarrow 0.011$ as $L/r_o \rightarrow \infty$ and $h_a(L/r_o) \rightarrow 0.067\ L/r_o \ln(L/r_o)$ as $L/r_o \rightarrow 0$. Kelman estimated that these formulae for the resistance give a maximum relative error of 0.0341 in the total current for a set potential difference between the counter and working electrodes. Kelman's estimated error translates into an absolute error for $h_a(L/r_o)$ of at least 0.0085, larger than or nearly as large as $h_a(L/r_o)$ itself.

Diem *et al.* [6] investigated the primary current distribution of the two-dimensional, recessed electrode shown in figure 2. The ratios of characteristic lengths that were held constant in their analysis are also shown. It can be seen that m/n is analogous to the aspect ratio L/r_o of the axisymmetric geometry. Their solutions should be quite accurate because conformal mapping procedures, which they used, account explicitly for the inherent singularities of the problem.

Small Aspect Ratios

In this section, we show how the current distribution and ohmic resistance can be estimated for recessed electrodes with very small aspect ratios. Away from the electrode/insulator edge, the current density is nearly indistiguishable from the current distribution valid for zero aspect ratio. Near the edge, the deviation from a zero aspect ratio has a major influence on the distribution. A singular-perturbation analysis in the aspect ratio can elucidate this behavior.

The region away from the edge will be referred to as the *outer region*. In the outer region, the current distribution for an isolated disk would be approximated by [7]

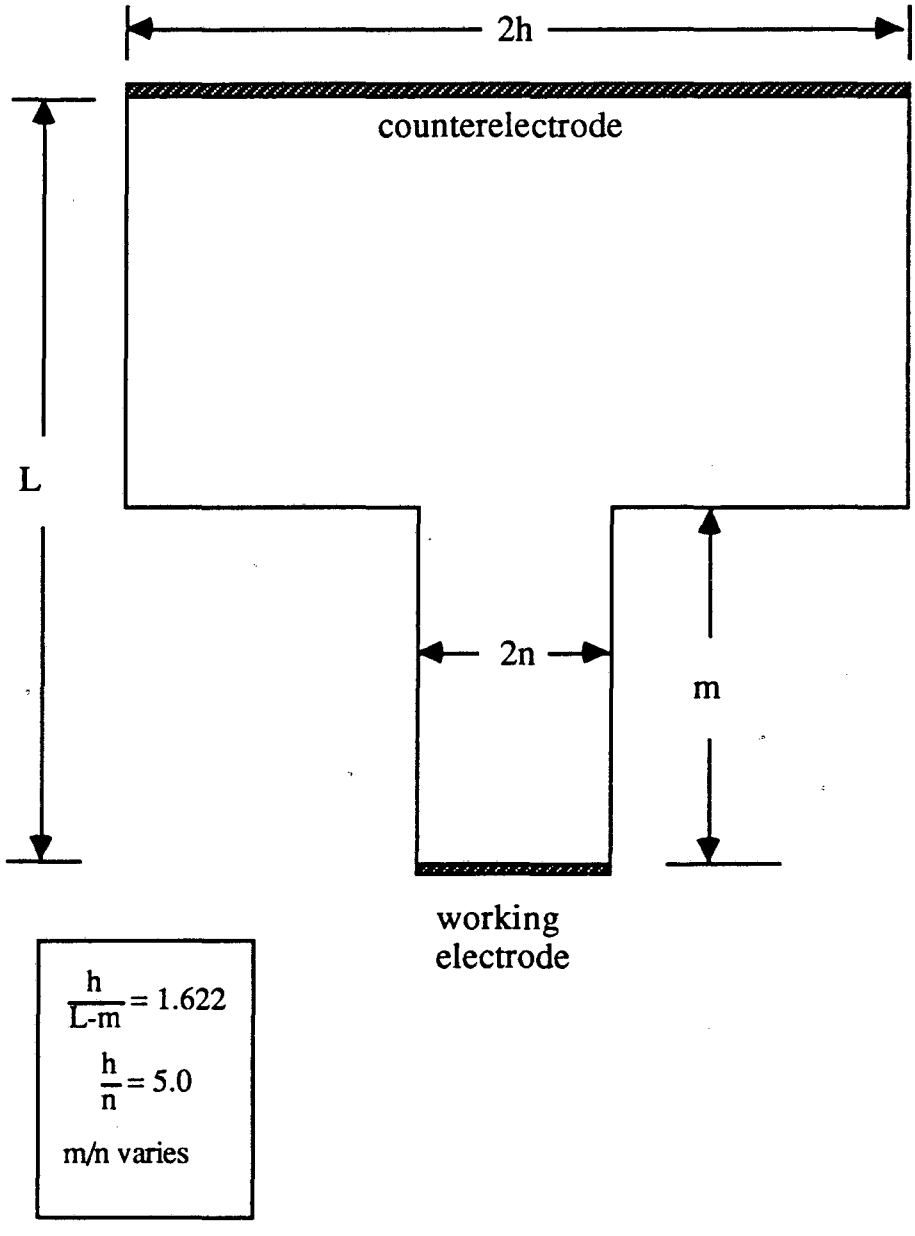

Figure 2. Two-dimensional, recessed electrode investigated by Diem *et al.* [6].

$$\frac{i(r)}{i_{avg}} = \frac{0.5}{(1 - r^2/r_o^2)^{1/2}}, \tag{10}$$

and, for a planar electrode with a counterelectrode placed at a distance very far from the working electrode [8],

$$\frac{i(x)}{i_{avg}} = \frac{2/\pi}{(1 - x^2/n^2)^{1/2}}. \tag{11}$$

Near the edge, the behavior of both current distributions is the same:

$$\lim_{\rho \to 0} i(\rho) = P_o/\sqrt{\rho}. \tag{12}$$

For a disk electrode, $P_o = \sqrt{r_o/8}\ i_{avg}$, and for an isolated, planar electrode, $P_o = (\sqrt{2n}/\pi)\ i_{avg}$. For the cell shown in figure 2, the value of the coefficient for P_o will differ slightly from the value for an isolated, planar electrode.

In the inner region, the counterelectrode placement and the details of the geometry influence the current distribution only through P_o. In this region, the geometry can be approximated by figure 3a, with a counterelectrode placed at a distance very far from the working electrode. Conformal mapping techniques are, therefore, ideal for this problem. The current distribution on the electrode is described by

$$-\kappa \frac{\partial \Phi}{\partial \bar{y}} = \frac{\sqrt{\pi L/2}\ P_o}{\sqrt{1 - u}}, \tag{13}$$

where the coordinates are shown in figure 3 and w and z are related through

$$\bar{z} = \frac{z}{L} = \frac{2}{\pi} \frac{w\sqrt{w-1}}{\sqrt{w}} + \frac{1}{\pi} \ln\left(\frac{\sqrt{w-1} - \sqrt{w}}{\sqrt{w-1} + \sqrt{w}}\right). \tag{14}$$

The coefficient of equation (13) was determined by matching with equation (12). To apply equations (13) and (14) to the two-dimensional

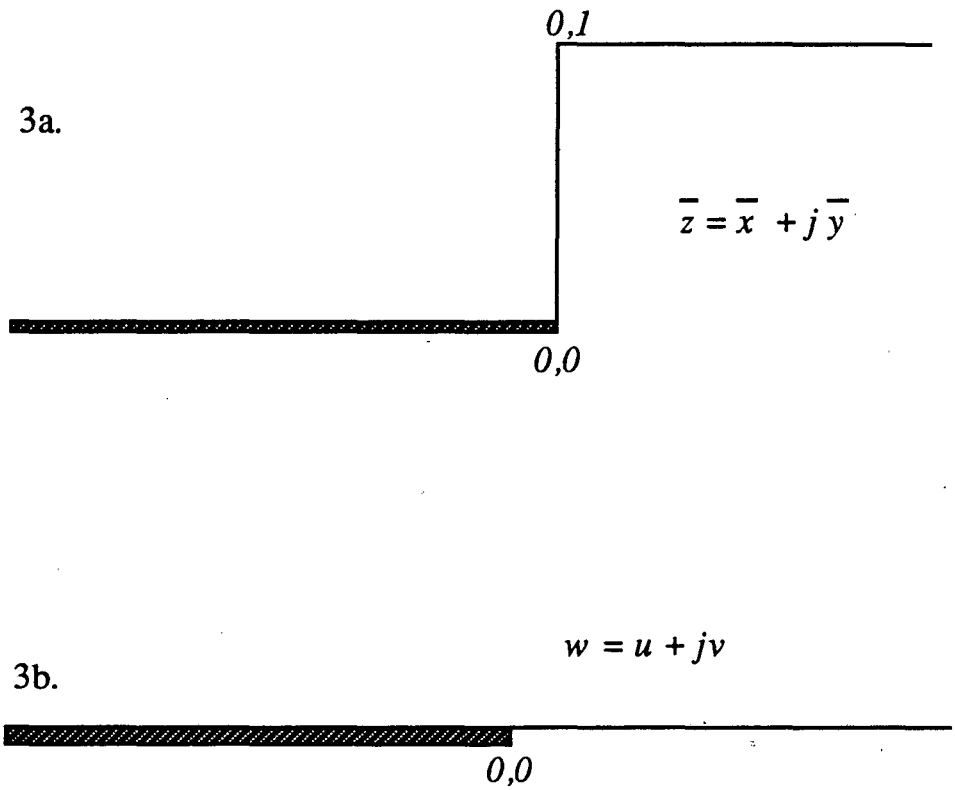

Figure 3. The original and transformed coordinate systems used to elucidate the current distribution near the edge of a recessed electrode for small aspect ratios. The mapping is achieved by requiring that

$$\frac{d\bar{z}}{dw} = \frac{2}{\pi}\frac{\sqrt{w\text{-}1}}{\sqrt{w}}.$$

cell, L should be replaced with m.

The above analysis shows that the current distribution near the edge is inversely proportional to the square root of the aspect ratio. For the disk electrode,

$$\frac{i_{edge}}{i_{avg}} = \frac{\sqrt{\pi}}{4} \sqrt{r_o/L}, \tag{15}$$

and, for the isolated, planar electrode,

$$\frac{i_{edge}}{i_{avg}} = \frac{1}{\sqrt{\pi}} \sqrt{n/m}. \tag{16}$$

Equation (16) can be verified by the complete analysis of a recessed planar electrode, given in the appendix. Figure 4 uses equations (13) and (14) to show how the current distribution near the edge of the disk deviates from the distribution valid for $L/r_o = 0$. Relative to the latter case, current is deflected from the edge region by the lip, but it still reaches the disk at a position somewhat away from the edge.

Numerical Analysis

Axisymmetric boundary integral equations were used to solve for the current distribution on the recessed disk. The problem was solved as one with a prescribed current distribution. Corresponding distributions of potential were superimposed until a constant potential on the disk was achieved.

The current distributions that were superimposed are

$$\frac{\partial \Phi}{\partial z} = P_{2n}\left[\sin\left[\frac{\pi r}{2r_o}\right]\right], \tag{17}$$

where P_{2n} are the even Legendre polynomials. It was found that the

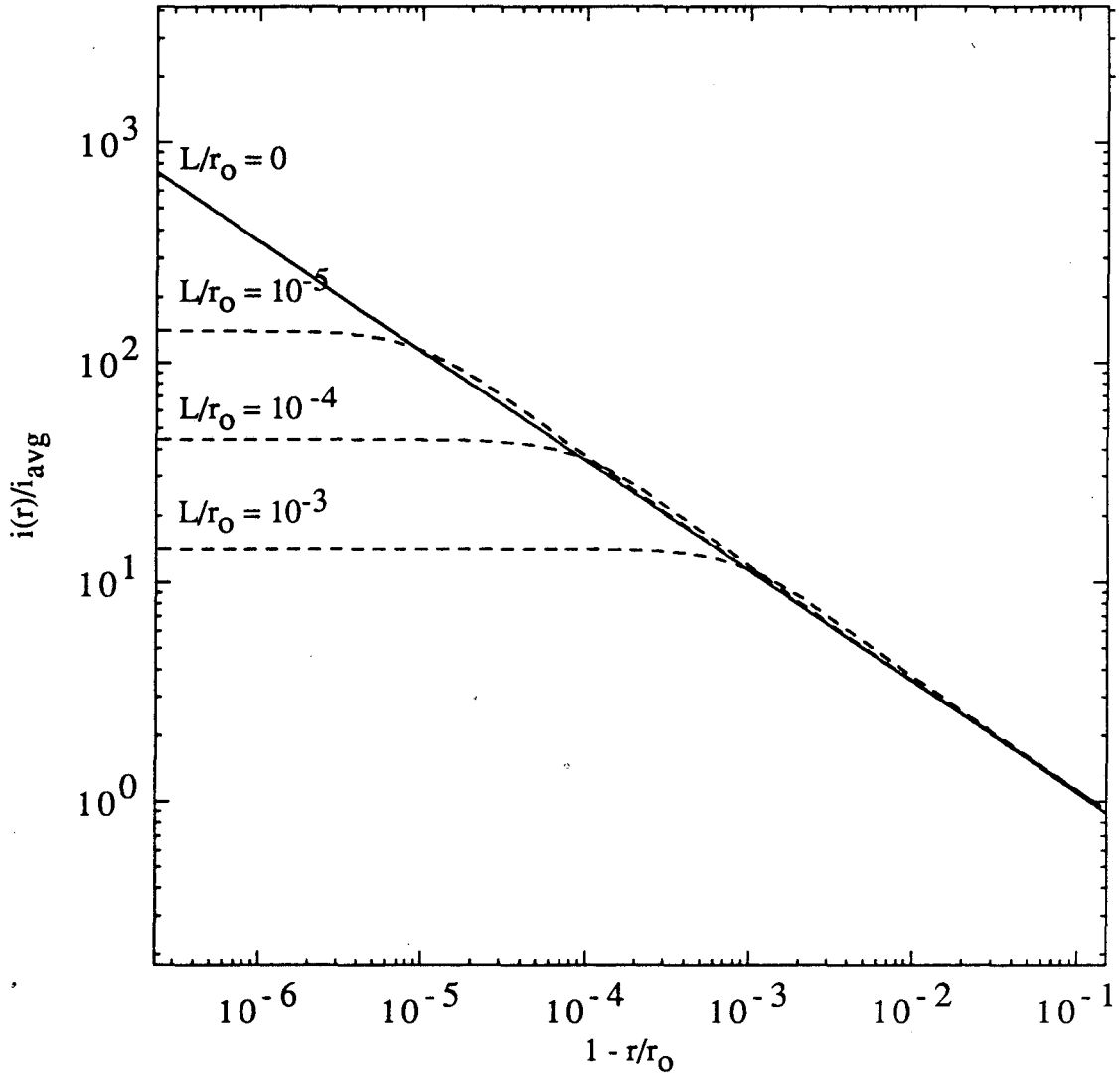

Figure 4. The distribution of current density, valid for small aspect ratios, near the edge of a recessed disk. The dashed lines were obtained from equations (13) and (14), and the solid line is the primary current distribution for a disk electrode, as given by equation (10).

polynomials from $2n = 0$ to $2n = 24$ were sufficient. Additional polynomials did not change appreciably the distribution. The argument for the polynomials is chosen so that the radial derivative of the current density is zero at the center and edge of the electrode. The recurrence formula used to evaluate the polynomials can be found in references [9] and [10], for example. To provide a check on our choice of current distributions, we also used the functions suggested by equation (8). The answers were essentially unchanged.

For this cell geometry, other techniques for determining the current density on an electrode with a constant potential boundary condition might give accurate solutions. For cells with obtuse angles of intersection between the electrode and insulator, the infinite current densities that arise can not be calculated accurately unless the correct form of the singularity is imbedded into the problem. Miksis and Newman [11] and Pierini and Newman [12] followed this procedure.

For small aspect ratios, the numerical technique discussed above fails to give reliable solutions. By using the results of the previous section it is possible to develop a modified procedure that allows for an accurate solution. Since the important features of the current distribution and ohmic resistance are elucidated by the perturbation analysis, we did not feel that it was necessary to devote more effort to the numerical calculations.

Results and Discussion

Figure 5 shows current distributions on a recessed disk for various aspect ratios. The dashed line is an approximation given by the composite solution obtained from the perturbation analysis:

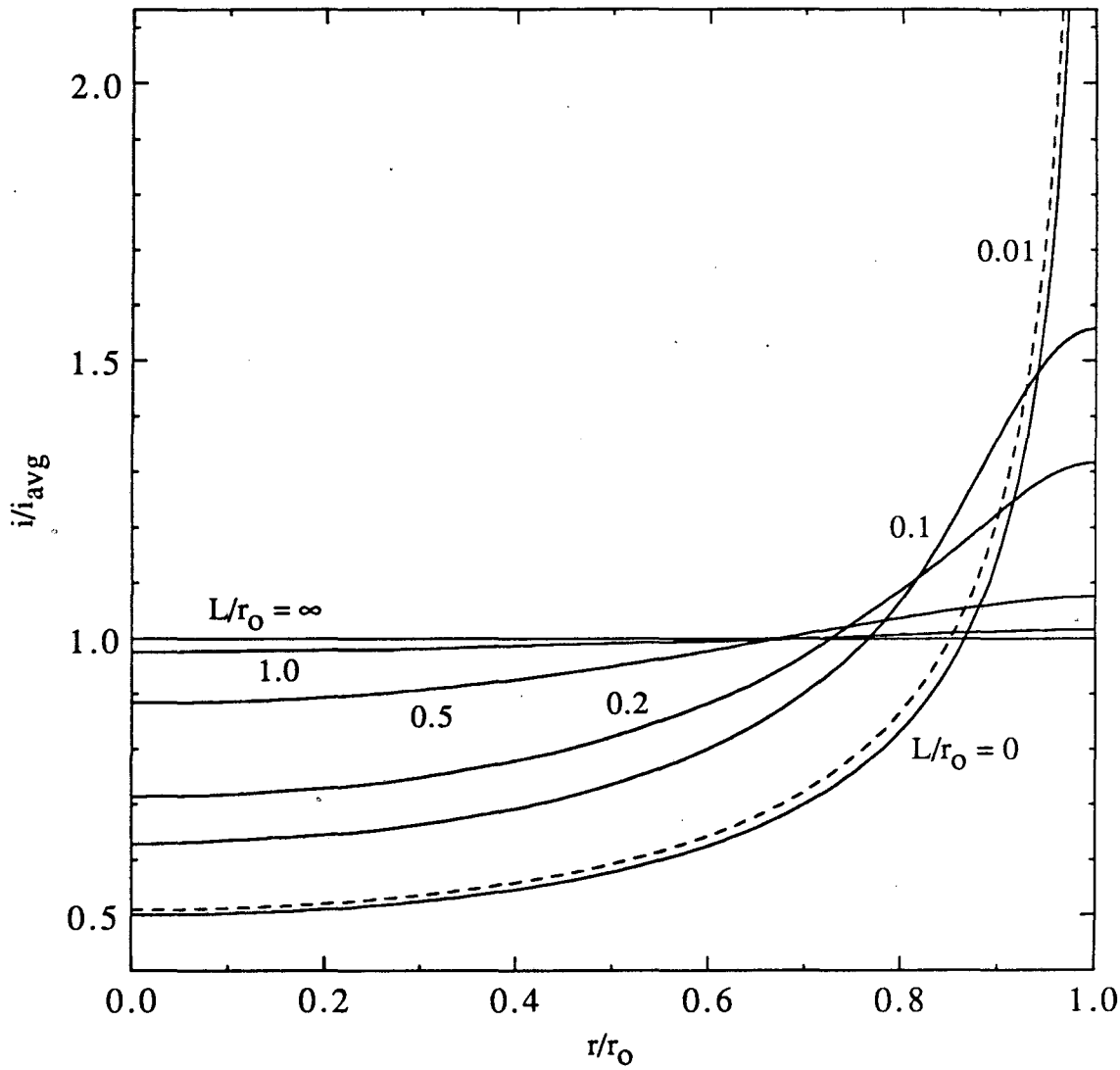

Figure 5. The primary current distribution on a recessed disk electrode for various values of the aspect ratio as determined by the numerical procedure. The current distribution given for an aspect ratio of 0.01 (the dashed line) is estimated from the perturbation analysis.

$$\frac{i(r)}{i_{avg}} = \left[\frac{0.5}{(1 - r^2/r_o^2)^{1/2}} + \frac{\sqrt{\pi}}{4}\frac{\sqrt{r_o/L}}{\sqrt{1-u}} - \frac{0.5}{\sqrt{2}(1 - r/r_o)^{1/2}}\right](1 - \epsilon)^{-1}, \quad (18)$$

where $1 - \epsilon$ arises because the ohmic resistance of the cell changes. It is the correction to the average current from the case when $L/r_o = 0$. It can be shown that

$$\epsilon = \int_0^{r_o}\left[-\frac{\sqrt{\pi}}{4}\frac{\sqrt{r_o/L}}{\sqrt{1-u}} + \frac{0.5}{\sqrt{2}(1 - r/r_o)^{1/2}}\right]rdr. \quad (19)$$

When $L/r_o = 0.01$, $\epsilon = 0.012$. Appendix B shows that the correction to the current density away from the edge region should be of the order $(L/r_o)\ \ln(L/r_o)$ for small aspect ratios.

Figure 6 gives the current density at the edge of the disk as a function of the aspect ratio. The dashed line is the prediction of the perturbation analysis, the solid line represents the case when $i_{edge} = i_{avg}$, and the points are the results of the numerical analysis. This figure indicates when the current distribution will be uniform. Slow electrode kinetics will make the current density on the electrode yet more uniform, and when concentration variations are important, convection will further distort the results.

Figure 7 shows the correction to the estimate of the ohmic resistance, defined by equation (5). The curve represents the different asymptotic formulae of Kelman, and the points are the result of the numerical analysis. For $L/r_o = 10.0$, we calculated that $h_a(L/r_o) = 0.011$, in agreement with the prediction of Kelman. Appendix B shows that $h_a(L/r_o) \propto (L/r_o)\ \ln(L/r_o)$ as $L/r_o \rightarrow 0$, also in agreement with the analysis of Kelman. Figure 7 shows that this correction is relatively unimportant since the maximum relative error in the resistance, when

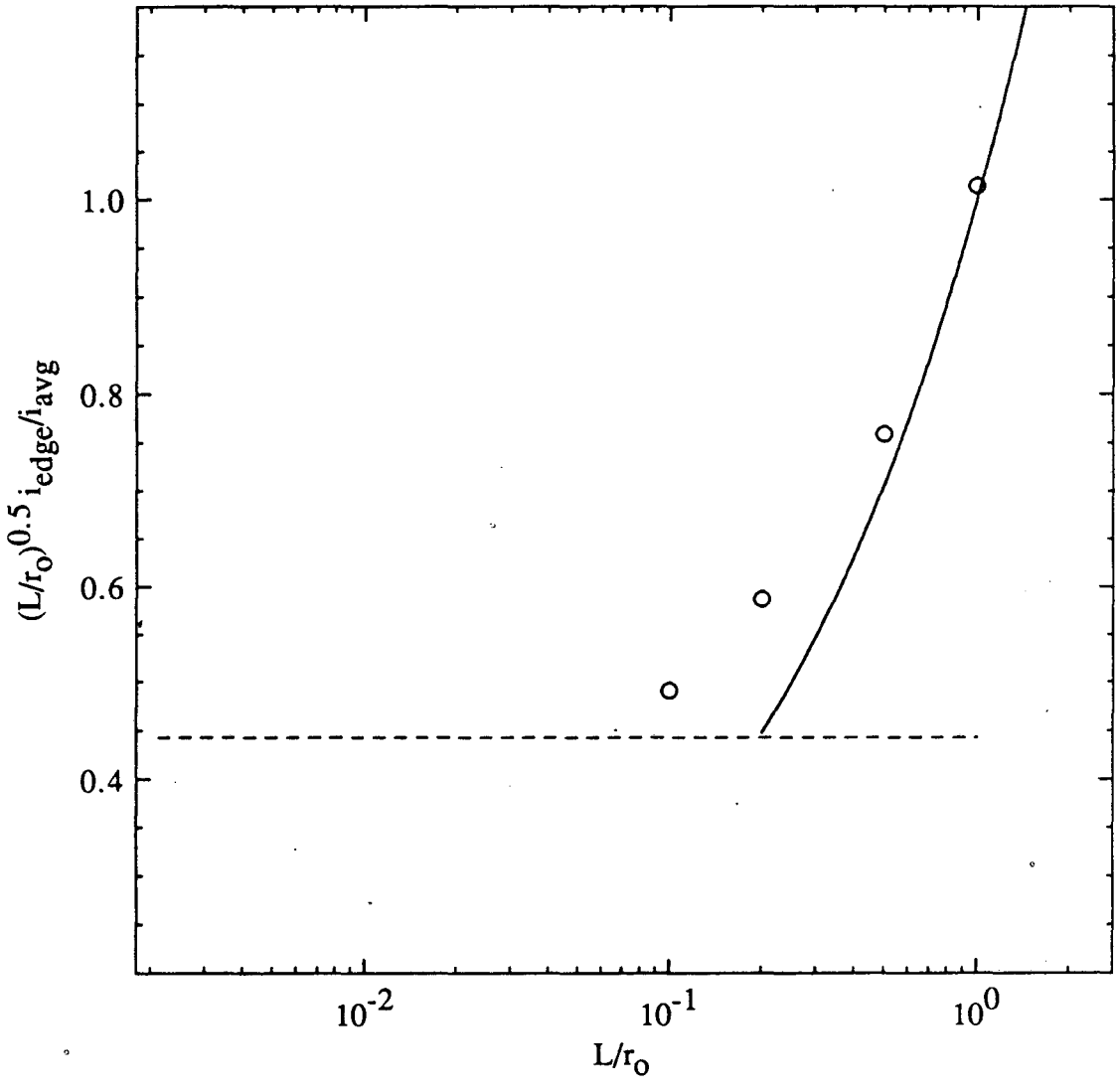

Figure 6. The current distribution on the edge of a recessed, disk electrode as a function of the aspect ratio. The dashed line is the asymptotic prediction for small aspect ratios, and the solid curve is the asymptotic prediction for large aspect ratios, which assumes that $i_{edge} = i_{avg}$.

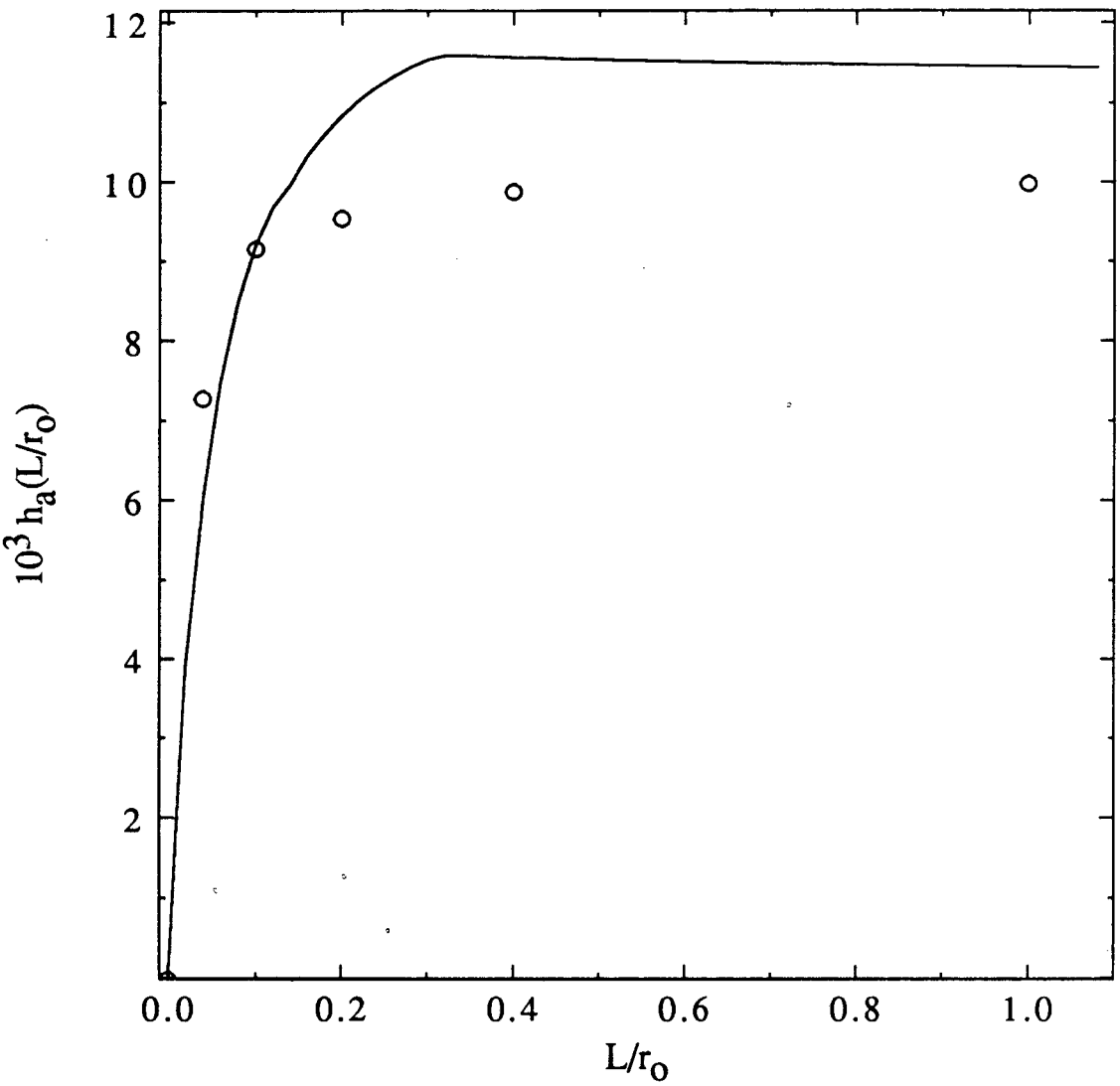

Figure 7. A correction to an estimation of the ohmic resistance of a recessed disk electrode as calculated by Kelman's formulae [4,5] and by the numerical procedure (open circles).

predicted by the first two terms of equation (5), is estimated to be 0.03 and occurs near $L/r_o = 0.1$.

Conclusions

The primary current distribution and ohmic resistance for various aspect ratios are given. The results can be used to design a cell that would have an approximately uniform current distribution in the absence of concentration variations. With convection, the mass-transfer limited current distribution can be nonuniform.

Appendix A

Figure A.1 shows the conformal mappings that determine the current distribution on a recessed, planar electrode with a counterelectrode placed essentially at infinity. The constants a and C are determined through

$$m = C \int_1^{1+a} \left[\frac{(1+a)^2 - w^2}{w^2 - 1} \right]^{1/2} dw \qquad (A.1)$$

and

$$n = C\,(1+a)\,E[(1+a)^{-2}], \qquad (A.2)$$

where $E[(1+a)^{-2}]$ is the complete elliptic integral of the second kind, as defined in reference [13]. For small aspect ratios, these equations become

$$m = \frac{\pi}{2}\,aC \qquad (A.3)$$

and

$$n = C\left(1 - \frac{a}{2}\ln a\right). \qquad (A.4)$$

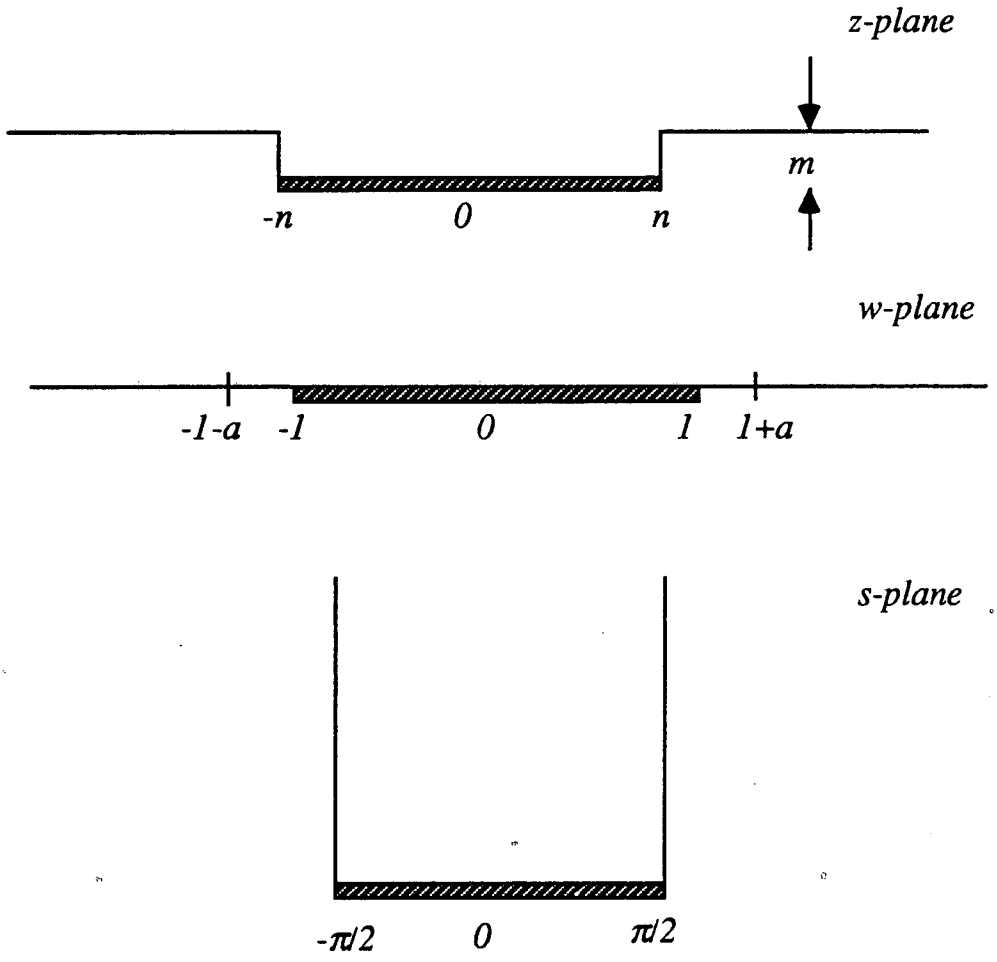

$$\frac{dz}{dw} = C \frac{\sqrt{w-1-a}\,\sqrt{w+1+a}}{\sqrt{w-1}\,\sqrt{w+1}}$$

$$w = \sin(s)$$

Figure A.1. A schematic of the mappings used to determine the ohmic resistance of a recessed, planar electrode, with a counterelectrode placed at a distance very far from the working electrode. Also shown are the coordinate transformations that provide the mappings. The constants a and C are determined as described in the text.

The current distribution can be written as

$$\frac{i(x/n)}{i_{avg}} = \frac{1}{C} \frac{2/\pi}{((1+a)^2 - w_r^2)^{1/2}}, \tag{A.5}$$

where x and w_r are related through the equation given in figure A.1. Equation (A.5), evaluated at $x = n$, is shown in figure A.2 as a function of m/n. The dashed line represents the prediction of equation (16).

An equation analogous to equation (5) can be written for this two-dimensional cell:

$$W\kappa R = W\kappa R_o + \frac{m}{2n} + h_2(m/n), \tag{A.6}$$

where W is the width of the electrode (perpendicular to figure A.1) and $W\kappa R_o$ is the resistance of the cell when $m/n = 0$. Figure A.3 shows $h_2(m/n)$, which is given by

$$h_2(m/n) = -\frac{1}{\pi} \ln C - \frac{m}{2n} . \tag{A.7}$$

For small m/n,

$$h_2(m/n) = -\frac{1}{\pi^2} \frac{m}{n} \ln(m/n), \tag{A.8}$$

and, for large m/n, $h_2(m/n) = 0.0208$. Equation (A.8) also applies to the cell shown in figure 2 when m/n is small.

Appendix B

The order of the next term, for either the potential or current density, in the outer region for the disk geometry is shown to be $(L/r_o) \ln(L/r_o)$. For a given electrode potential, the value of $h_a(L/r_o)$ comes, indirectly, from an integration of the average current density over the surface of the disk. The fact that the correction of the current density in the edge region is $O(\sqrt{r_o/L})$ and the size of this

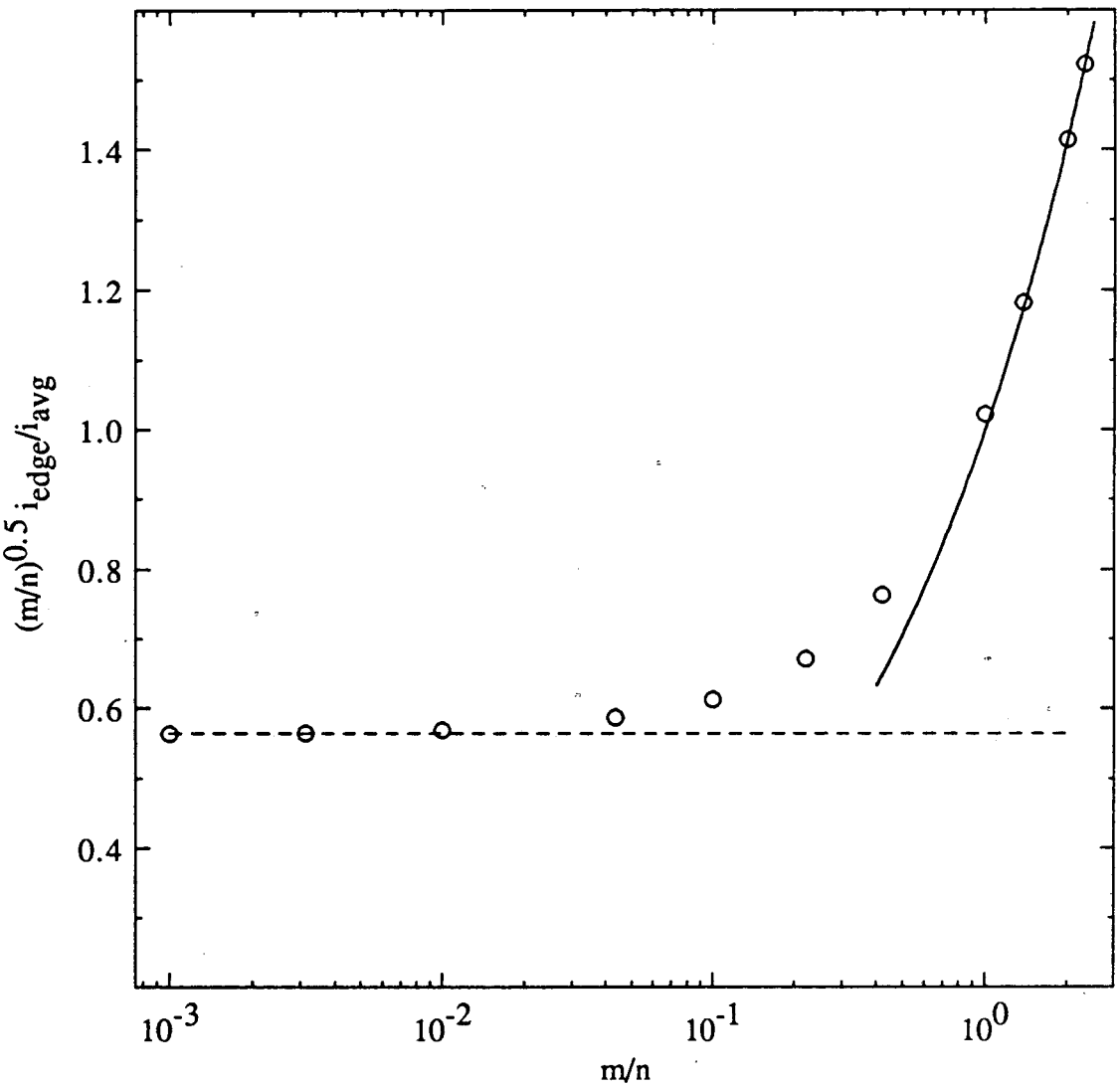

Figure A.2. The current distribution on the edge of a recessed, planar electrode as a function of the aspect ratio m/n. The dotted line is the asymptotic prediction for small aspect ratios, and the solid curve is the asymptotic prediction for large aspect ratios, which assumes that $i_{edge} = i_{avg}$.

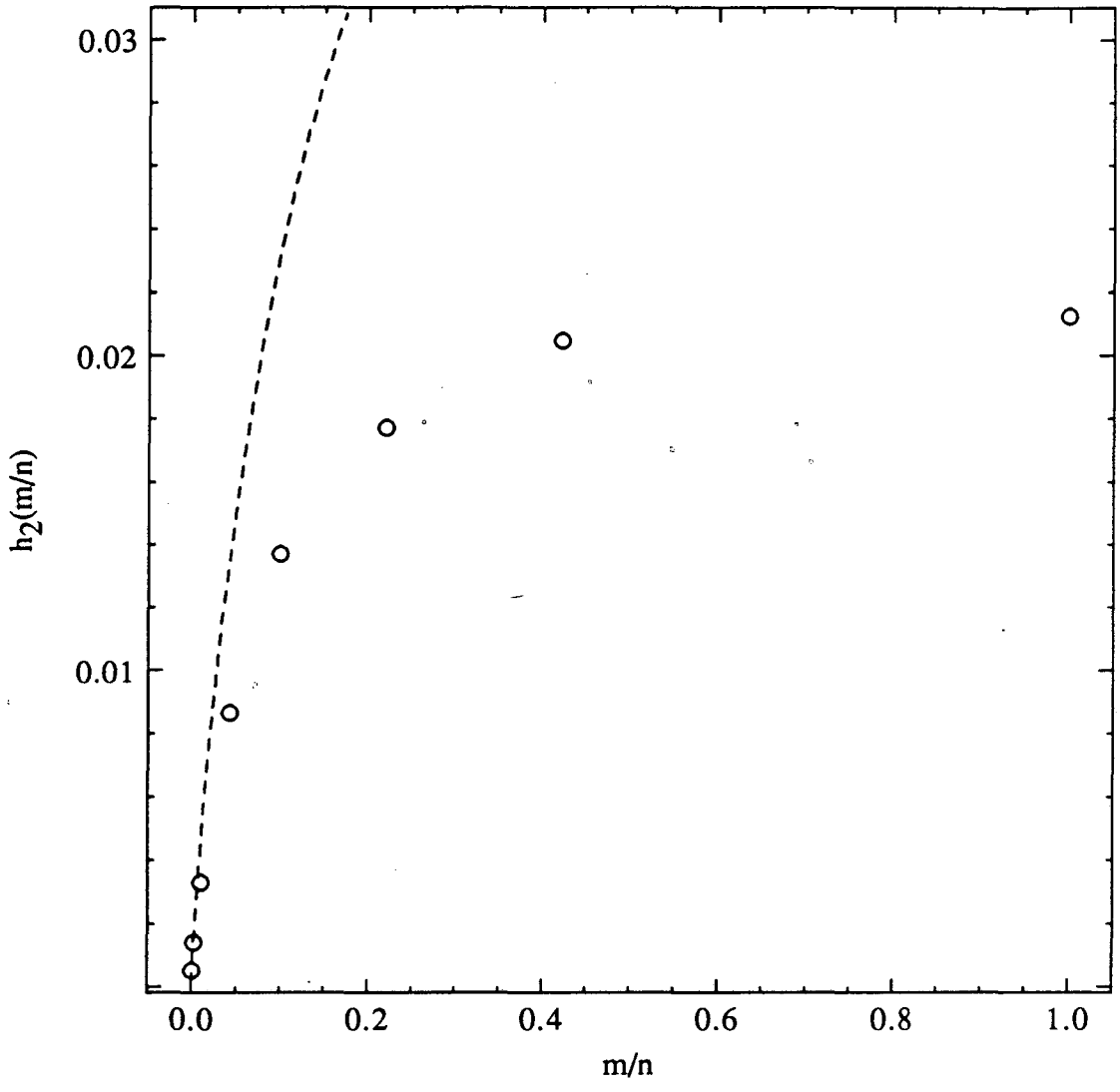

Figure A.3. The correction to the ohmic resistance of the recessed, planar electrode as a function of the aspect ratio *m/n*, as given by equation (A.7). The dashed line is the asymptotic limit valid for small aspect ratios.

region is $O(L/r_o)$ might suggest that the edge region would lead to a correction $h_a(L/r_o)$ of $O(\sqrt{L/r_o})$. However, the current deflected from the edge itself mostly reaches the disk but is displaced inward from the edge (see figure 4). Consequently, the order of the first term describing $h_a(L/r_o)$ is obtained from the outer region and is also of order $(L/r_o)\ \ln(L/r_o)$.

The next term in a perturbation analysis arises from previously neglected terms in the matching conditions, boundary conditions, or governing equations. In the outer region, no terms were neglected in Laplace's equation. Since the electrode boundary condition was imposed at a position coplanar with the insulating plane, this boundary condition was not strictly satisfied. The term arising from this discrepancy can be shown to be of the order L/r_o. A larger term, though, arises from the matching condition.

The potential in the inner region can be expanded formally as

$$\bar{\phi} = \sqrt{r_o/L}\ \frac{\Phi}{V} = \bar{\phi}^{(0)} + \bar{f}_1(L/r_o)\ \bar{\phi}^{(1)} + \ \ldots\ , \tag{B.1}$$

and the potential in the outer region as

$$\bar{\phi} = \frac{\Phi}{V} = \bar{\phi}^{(0)} + \bar{f}_1(L/r_o)\ \bar{\phi}^{(1)} + \ \ldots\ . \tag{B.2}$$

The matching condition for these two series is

$$\sqrt{L/r_o}\ \bar{\phi}(\bar{x}^2+\bar{y}^2 \longrightarrow \infty) = \bar{\phi}(\xi \longrightarrow 0, \eta \longrightarrow 0), \tag{B.3}$$

where η and ξ are rotational elliptic coordinates, given by

$$z = r_o \xi \eta, \tag{B.4}$$

and

$$r = r_o \left((1+\xi^2)(1-\eta^2)\right)^{1/2}. \tag{B.5}$$

Newman [7] gave the first term of the outer expansion:

$$\bar{\phi}^{(0)} = \frac{2}{\pi} \tan^{-1}\xi. \tag{B.6}$$

The first term of the inner expansion is

$$\bar{\phi}^{(0)} = \frac{2\sqrt{2}}{\pi^{3/2}} (\rho_w + u)^{1/2}, \tag{B.7}$$

where $\rho_w = (u^2 + v^2)^{1/2}$ and u and v are the coordinates described in figure 3. Equation (B.7), when expanded for large w and related to the outer variables, becomes

$$\bar{\phi}^{(0)}(\bar{x}^2+\bar{y}^2 \longrightarrow \infty) = \frac{2}{\pi} \sqrt{r_o/L}\ (\rho + x)^{1/2} \tag{B.8}$$

$$+ \frac{1}{\pi^2} \sqrt{L/r_o}\ \ln(L/r_o)\ \frac{(\rho + x)^{1/2}}{\rho^{3/2}} + O[(L/r_o)^{1/2}].$$

The outer solution for small ξ and η, is

$$\bar{\phi}(\eta\longrightarrow 0, \xi\longrightarrow 0) = \frac{2}{\pi}\,\xi = \frac{2}{\pi}\,(\rho + x)^{1/2} + O[\rho^{1/2}], \tag{B.9}$$

where $\rho = (x^2 + y^2)^{1/2}$ (see figure 3). The leading terms of the inner and outer expansions are matched. The second term on the right of equation (B.8) must be matched by $\bar{\phi}^{(1)}$, which implies that $\bar{f}_1(L/r_o) = (L/r_o)\ \ln(L/r_o)$.

Acknowledgements

This work was supported by the Assistant Secretary for Conservation and Renewable Energy, Office of Energy Storage and Distribution, Energy Storage Division, of the U. S. Department of Energy under Contract No. DE-AC03-76SF00098.

List of Symbols

A_n, B_n	coefficients in a series
$h_a(L/r_o)$	correction to estimate of axisymmetric cell resistance
$h_2(m/n)$	correction to estimate of two-dimensional cell resistance
i	current density, A/cm^2
J_o	Bessel function of the first kind of order zero
L	depth of recess, cm
m/n	ratio of lengths
P_{2n}	even Legendre polynomials
r, z	cylindrical coordinates
r_o	radius of the disk electrode, cm
R	cell resistance, ohm
V	electrode potential, V
η, ξ	rotational elliptic coordinates
κ	specific conductivity, $\Omega^{-1}cm^{-1}$
π	3.141592654
ρ, θ	cylindrical coordinates used near $r = r_o$, $z = L$
Φ	solution potential, V

Subscripts

avg	average
center	center
edge	edge
q	denotes a point at which the potential is solved

References

[1] Theodore R. Beck, "Formation of Salt Films during Passivation of Iron," *J. Electrochem. Soc.*, 129, 2412 (1982).

[2] James Clerk Maxwell, *A Treatise on Electricity and Magnetism*, vol. 1, pp 431-434, 3rd edition, Clarendon Press, Oxford (1904).

[3] John William Strutt Rayleigh, *Theory of Sound*, vol. 2, pp. 487-491, republication of the 2nd edition, Dover, New York (1926).

[4] R. B. Kelman, "Axisymmetric Potentials in Composite Geometries: Finite Cylinder and Half Space," *Contr. Diff. Eqs.*, 2, 421 (1963).

[5] R. B. Kelman, "Steady-State Diffusion Through a Finite Pore into an Infinite Reservoir: An Exact Solution," *Bull. Math. Biophysics*, 27, 57 (1965).

[6] Conrad B. Diem, Bernard Newman, and Mark E. Orazem, "The Influence of Small Machining Errors on the Primary Current Distribution at a Recessed Electrode," *J. Electrochem. Soc.*, 135, 2524 (1988).

[7] John Newman, "Resistance for Flow of Current to a Disk," *J. Electrochem. Soc.*, 113, 501 (1966).

[8] Carl Wagner, "Theoretical Analysis of the Current Density Distribution in Electrolytic Cells," *J. Electrochem. Soc.*, 98, 116 (1951).

[9] Francis B. Hildebrand, *Advanced Calculus for Applications*, p. 158, Prentice-Hall, Inc., Englewood Cliffs, N. J. (1976).

[10] M. Abramowitz and I. Stegun, *Handbook of Mathematical Functions*, p. 333, National Bureau of Standards, Washington (1964).

[11] Joseph J. Miksis, Jr., and John Newman, "Primary Resistances for Ring-Disk Electrodes," *J. Electrochem. Soc.*, 123, 1030 (1976).

[12] Peter Pierini and John Newman, "Potential Distribution for Disk Electrodes in Axisymmetric Cylindrical Cells," *J. Electrochem. Soc.*, 122, 1348 (1979).

[13] M. Abramowitz and I. Stegun, *ibid.*, p. 589.

LAWRENCE BERKELEY LABORATORY
TECHNICAL INFORMATION DEPARTMENT
1 CYCLOTRON ROAD
BERKELEY, CALIFORNIA 94720